

XVI. PLASMA MAGNETOHYDRODYNAMICS AND ENERGY CONVERSION*

Prof. E. N. Carabateas	R. S. Cooper	A. T. Lewis
Prof. J. A. Fay	F. W. Fraim III	J. R. Melcher
Prof. S. I. Freedman	N. Gothard	H. D. Meyer
Prof. G. N. Hatsopoulos	C. W. Haldeman	W. T. Norris
Prof. W. D. Jackson	H. M. Heggstad	J. H. Olsen
Prof. H. P. Meissner	W. H. Heiser	E. S. Pierson
Prof. P. L. Penfield, Jr.	J. B. Heywood	J. W. Poduska
Prof. J. P. Penhune	E. D. Hoag	D. H. Pruslin
Prof. D. C. Pridmore-Brown	P. G. Katona	A. R. Reti
Prof. A. H. Shapiro	F. D. Ketterer	C. W. Rook
Prof. J. L. Smith, Jr.	G. B. Kliman	A. Shavit
Prof. H. H. Woodson	P. Klimowski	J. H. Sumunu
J. B. Bledsoe	A. G. F. Kniazzeh	R. G. Vanderweil
J. L. Coggins	M. F. Koskinen	E. F. Wahl III
J. B. Conklin, Jr.	W. H. Levison	G. L. Wilson

RESEARCH OBJECTIVES

1. Plasma Magnetohydrodynamics

The general purpose of the magnetohydrodynamic research is to explore interaction phenomena in those situations in which the fluid can be considered to be predominantly a continuum. This includes a wide range of phenomena, from the flow of liquid metals through magnetic fields to the propagation of hydromagnetic shock waves. At the present time, we are exploring such problems as boundary-layer flow over a flat plate with normal magnetic field, the flow over pitot tubes in the presence of a magnetic field, the confinement of dense plasmas with dc and ac magnetic fields, the acceleration of plasmas by $J \times B$ forces, and the propagation of disturbances in a medium containing a magnetic field.

While some of the experimental work is concerned with liquid metals, a large proportion makes use of shock tubes to produce high-velocity plasmas whose interactions with magnetic fields can be studied. One of our research objectives is to extend these techniques to include a greater range of physical parameters.

J. A. Fay

2. Energy Conversion

(a) Magnetohydrodynamic Energy Conversion

The objectives in this area are twofold:

(i) To study problems of magnetohydrodynamic flow in order to obtain a better understanding of the many phenomena involved, such as turbulence and wave motion. This involves both theoretical and experimental work.

(ii) To study systems in which energy conversion can occur between flow energy in a conducting liquid or gas and an electrical system. The systems of interest include steady and nonsteady fluid flow, and dc and ac electrical systems. The work involves theoretical and experimental evaluation of magnetohydrodynamic conversion schemes.

H. H. Woodson, W. D. Jackson

* This work was supported in part by the National Science Foundation under Grant G-9330, and in part by the U.S. Air Force (Aeronautical Systems Division) under Contract AF33(616)-7624 with the Flight Accessories Laboratory, Wright-Patterson Air Force Base, Ohio.

(XVI. PLASMA MAGNETOHYDRODYNAMICS)

(b) Thermionic Energy Conversion

Present objectives lie in four distinct areas of direct thermionic energy conversion. The first relates to the theoretical study of the Richardson equation by means of irreversible thermodynamics; the second, to experimental verification of the Saha-Langmuir equation in the region of partial coverage; the third, to the theoretical and experimental analysis of plasmas and sheaths; and the fourth, to the correlation of the effect of emitter work function on the efficiency and ion production rate of cesium converters while operating in the neutralized space-charge region.

G. N. Hatsopoulos, E. N. Carabateas

(c) Fuel Cells

Our objective is to learn more about the mechanism of the various chemical, physical and electrochemical processes that occur simultaneously in a fuel cell. Studies will be directed toward satisfying the criteria of high electrode current density and high efficiency in low-temperature, low-pressure fuel cells that are capable of operating on air and hydrogen and commonly available hydrocarbons.

H. P. Meissner

A. REFLECTION AND REFRACTION OF MAGNETOACOUSTIC WAVES AT AN INTERFACE

The linearized equations describing the propagation of small disturbances in a compressible continuous and dissipation-free fluid (zero viscosity and heat conductivity, infinite electrical conductivity) that is immersed in a uniform magnetic field \vec{B}_0 are:

$$\begin{aligned}\frac{\partial \rho}{\partial t} + \rho_0 \operatorname{div} \vec{v} &= 0 \\ \rho_0 \frac{\partial \vec{v}}{\partial t} + \operatorname{grad} p &= \frac{1}{\mu} (\operatorname{curl} \vec{B}) \times \vec{B}_0 \\ \frac{\partial \vec{B}}{\partial t} &= \operatorname{curl} (\vec{v} \times \vec{B}_0) \\ \frac{\partial}{\partial t} S(p, \rho) &= 0.\end{aligned}$$

These equations can be combined to give the following wave equation in the particle velocity \vec{v} ,

$$\frac{\partial^2 \vec{v}}{\partial t^2} = a^2 \operatorname{grad} \operatorname{div} \vec{v} + b^2 [\operatorname{curl} \operatorname{curl} (\vec{v} \times \vec{i})] \times \vec{i}$$

Here, $\vec{i} = \vec{B}_0 / |\vec{B}_0|$ is a unit vector in the direction of the imposed magnetic field, $a^2 = (\partial p / \partial \rho)_S$ is the acoustic speed, and $b^2 = B_0^2 / \rho \mu$ is the Alfvén speed. This wave equation is satisfied by plane waves propagating in an arbitrary direction at any of three different wave speeds c_f , c_i , and c_s , the subscripts standing for fast, intermediate, and slow. In terms of the fundamental wave speeds a and b and the angle θ between the wave normal and the magnetic field, these are given by

$$c_i = b \cos \theta$$

$$c_f^2 c_s^2 = a^2 b^2 \cos^2 \theta$$

$$c_f^2 + c_s^2 = a^2 + b^2.$$

In the intermediate wave the particle velocity is transverse to both the wave normal and the magnetic field, while in the other two it lies in the plane of these vectors.

It is interesting to enquire into the behavior of such waves on reflection at a plane interface between two media distinguished by different values of the undisturbed pressure, density, and magnetic field. We restrict ourselves to the cases in which the wave normal, the normal to the interface, and the magnetic field all lie in a plane.

Suppose, first, that the magnetic field is parallel to the interface. Then for static equilibrium any discontinuity in the magnetic field across the interface must be balanced by a corresponding discontinuity in the gas pressure so as to keep the total pressure $p_0 + B_0^2/2\mu$ continuous. Also, suppose that a fast wave is incident at an angle ϕ as illustrated in Fig. XVI-1. Such a wave will set up a ripple in the interface that will propagate to the right at a speed V_T equal to the trace velocity of the wave, which is

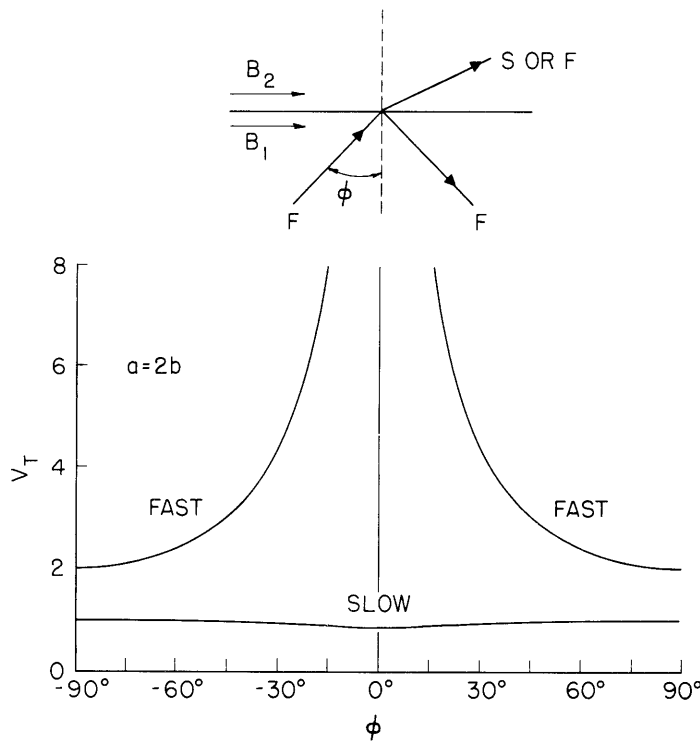


Fig. XVI-1. The trace velocity for fast and slow waves versus the angle of incidence when the magnetic field is parallel to the interface.

(XVI. PLASMA MAGNETOHYDRODYNAMICS)

$c_1/\sin \phi$. This ripple will then generate reflected and refracted waves at angles that are such that their trace velocities match the ripple speed. The trace velocity for both fast and slow waves is plotted in Fig. XVI-1 for $a = 2b$. From the graph it is clear that an incident fast wave will give rise to a reflected fast wave at an angle of reflection equal to the angle of incidence, and similarly for a slow wave. For the transmitted wave we see that if the ripple speed lies above a_2 (which is the greater of the two speeds a_2, b_2 in the second medium), then the transmitted wave will be fast regardless of the nature of the incident wave. Similarly, if it lies between b_2 and $a_2 b_2 / (a_2^2 + b_2^2)^{1/2}$, then the transmission wave will be slow. Finally, if it lies outside these ranges, there will be no transmitted wave; that is, the incidence wave will be totally reflected. An incident transverse wave will not set up a ripple in the interface (since its particle velocity is tangent to the interface) and thus cannot give rise to reflected and transmitted waves. In each case the relative amplitude of the reflected and transmitted waves, when they exist, can be found from the conditions of continuity of total pressure $p + B^2/2\mu$ and of the normal component of particle velocity.

Now suppose that the magnetic field is perpendicular to the interface. In this case the magnetic field and hence also the pressure must be continuous across it.

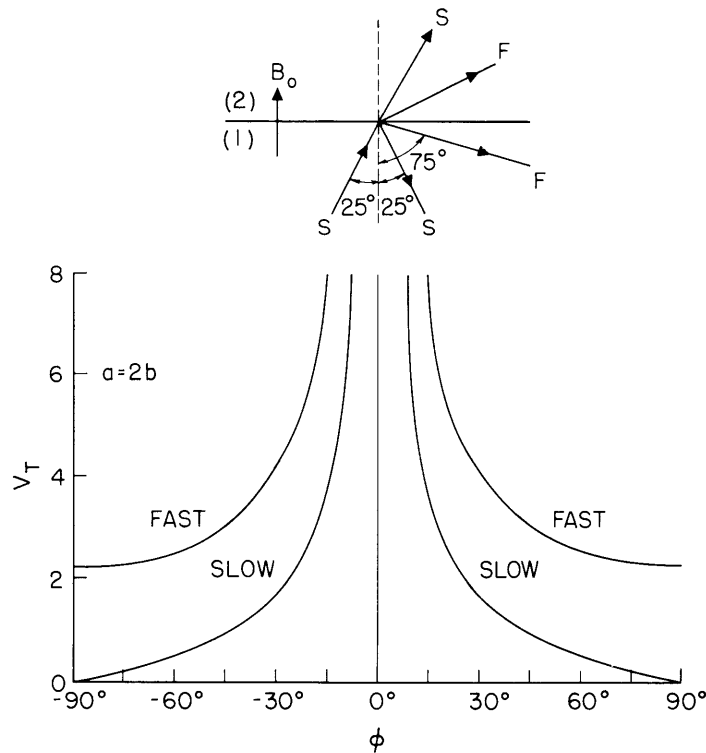


Fig. XVI-2. The trace velocity for fast and slow waves versus the angle of incidence when the magnetic field is perpendicular to the interface.

Figure XVI-2 illustrates the case for an incident slow wave. From the graph of trace velocity versus angle shown in Fig. XVI-2 it is clear that this wave can, in general, generate two reflected waves and two transmitted waves, one of each kind. Of the reflected waves, the slow one leaves at an angle of reflection equal to the angle of incidence, while the fast one leaves at a greater angle. If the angle of incidence exceeds a certain critical value, then the only reflected wave will be the slow one. Two reflected waves will, however, always be produced by an incident fast wave. The appearance of two transmitted and two reflected waves is not surprising when one considers that, in this case, in addition to continuity of total pressure and normal component of particle velocity one must also require continuity of the tangential component of particle velocity. This last requirement is necessary to ensure continuity of the tangential electric field. An incident intermediate wave gives rise simply to single reflected and transmitted waves of the same species. (The condition of continuous normal component of velocity is trivially satisfied in this case.)

Suppose, finally, that the magnetic field makes an angle of 45° with the interface. The magnetic field and pressure must again be continuous in this case, as in the last, since any discontinuity in the tangential component of B_0 would lead to an unbalanced

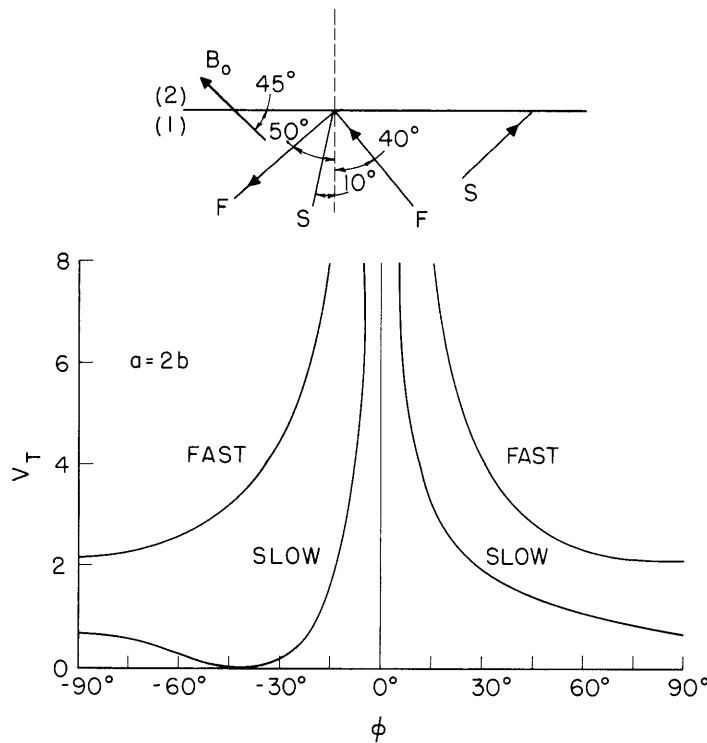


Fig. XVI-3. The trace velocity for fast and slow waves versus the angle of incidence when the magnetic field makes an angle of 45° with the interface.

(XVI. PLASMA MAGNETOHYDRODYNAMICS)

tangential stress in the interface. Figure XVI-3 shows that we again get two reflected and two transmitted waves generated by a single incident fast or slow wave. However, neither angle of reflection equals the angle of incidence, now. Also, for the incident slow wave there is now a critical angle above which the wave is totally transmitted; that is, the ripple is travelling too slowly to generate any reflected waves.

D. C. Pridmore-Brown

B. PARAMETRIC GENERATOR

In Quarterly Progress Report No. 63 (pages 49-55), a parametric generator system was described and preliminary data were presented which indicated that a circuit model for which parameters are derived from the results of steady-state ac measurements provides a good experimental basis on which to predict the performance of the system as a parametric generator. The purpose here is to present more extensive experimental evidence of the validity of the model under restricted conditions.

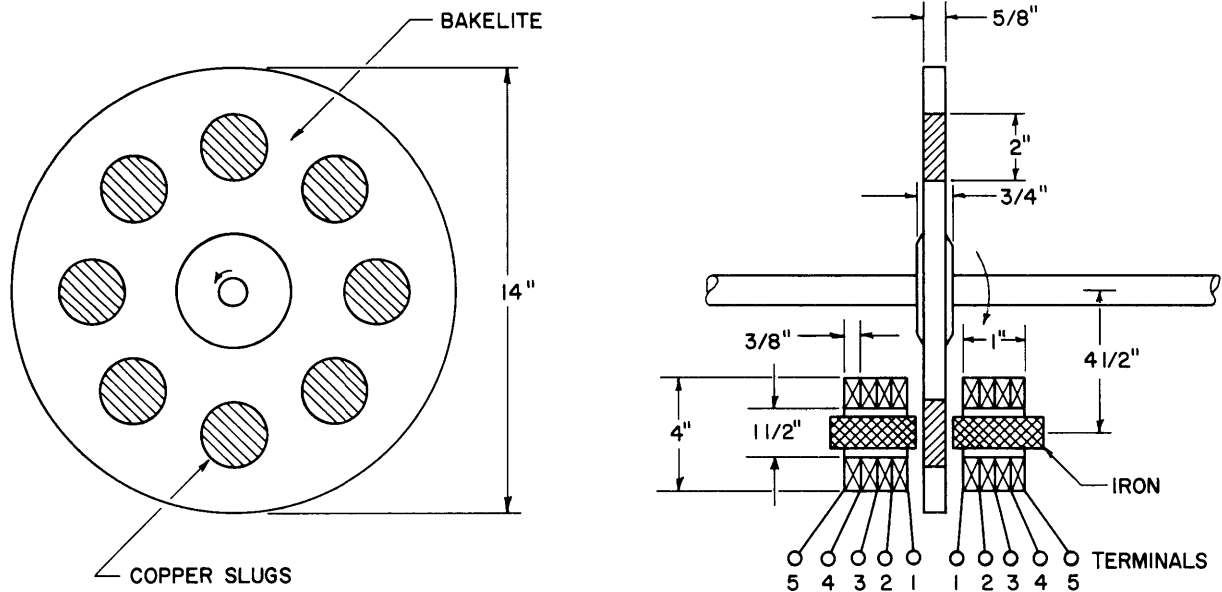


Fig. XVI-4. Two views of the wheel with the position of the new coils shown in the end view.

The parametric part of the system, shown in Fig. XVI-4, consists of a bakelite disc with 8 cylindrical copper slugs mounted symmetrically in it, and a pair of series-aiding coils with laminated iron cores. As the bakelite disc rotates, the copper slugs pass periodically between the coils, thereby causing the parametric variation.

(XVI. PLASMA MAGNETOHYDRODYNAMICS)

With the slugs traversing the coils at a radian frequency 2ω , circuit excitation at a frequency ω , a reciprocal inductance $(\Gamma_o + \Delta\Gamma \sin 2\omega t)$, and steady-state operation, the equivalent circuit derived previously is as shown in Fig. XVI-5. In the equivalent

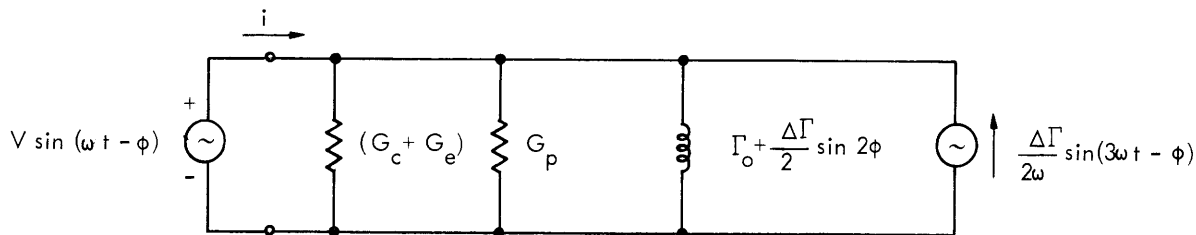


Fig. XVI-5. Steady-state equivalent circuit.

circuit, G_c represents coil and iron losses, G_e represents losses in the copper slugs, Γ_o is the average reciprocal inductance of the coil, $\Delta\Gamma$ is the change in reciprocal inductance caused by passage of the copper slugs between the coils, and G_p , the conductance caused by the parametric variation, is given by

$$G_p = -\frac{\Delta\Gamma}{2\omega} \cos 2\phi. \quad (1)$$

Self-excitation can occur when G_p is negative and larger in magnitude than $(G_c + G_e)$. This condition is expressible in terms of a parameter H , defined as

$$H = \frac{\Delta\Gamma}{2\omega(G_c + G_e)} \geq 1. \quad (2)$$

To determine how well the model predicts the onset of self-excitation, steady-state ac measurements were made with the wheel at rest for several different coil combinations at a frequency of 300 cps. These data were then used to determine the parameters of the equivalent circuit with the aid of the expressions

$$\Gamma_o = \frac{\Gamma_{\max} + \Gamma_{\min}}{2} \quad \Delta\Gamma = \frac{\Gamma_{\max} - \Gamma_{\min}}{2}$$

$$G_c = G_{\min} \quad G_e = \frac{G_{\max} - G_{\min}}{2}.$$

These data are given in Table XVI-1 with a calculation of the parameter H as given by Eq. 2. The wheel was then driven at the proper speed to make the slugs traverse the coil at a frequency of 600 cps, the coil was tuned to a frequency of 300 cps, and each coil configuration was tested for self-excitation. The results are given in Table XVI-1.

(XVI. PLASMA MAGNETOHYDRODYNAMICS)

Table XVI-1. Data taken at 300-cps frequency.

Coil Combination	Slug between Coils		Slug out of Coils		Γ_o (h ⁻¹)	$\Delta\Gamma$ (h ⁻¹)	G_c $\times 10^{-3}$ (mhos)	G_e $\times 10^{-3}$ (mhos)	H	Self-excited	
	Γ_{max} (h ⁻¹)	G_{max} $\times 10^{-3}$ (mhos)	Γ_{min} (h ⁻¹)	G_{min} $\times 10^{-3}$ (mhos)						Yes	No
1-2	43.6	6.5×10^{-3}	26.1	1.39	34.9	8.8	1.39	2.61	.51		✓
1-3	11.8	1.2×10^{-3}	7.4	.25	9.6	2.2	.25	.49	.79	✓	
1-4	5.0	.52	3.2	.08	4.1	.9	.08	.22	.88	✓	
1-5	2.8	.21	1.9	.04	2.3	.44	.04	.09	.93	✓	
2-3	41.3	4.58	28.9	1.51	35.1	6.2	1.51	1.54	.54		✓
2-4	9.7	.76	7.1	.22	8.4	1.3	.22	.27	.71		✓
2-5	4.4	.27	3.1	.08	3.8	.6	.08	.10	.94	✓	
3-4	31.8	2.81	24.5	1.36	28.1	3.6	1.36	.72	.46		✓
3-5	8.5	.52	6.6	.20	7.5	1.0	.20	.16	.70		✓
4-5	31.4	2.44	25.6	.64	28.5	2.9	.64	.90	.51		✓

This experiment was done with the circuit of Fig. XVI-6 in which the neon bulb limits voltage for protection of the self-excited system.

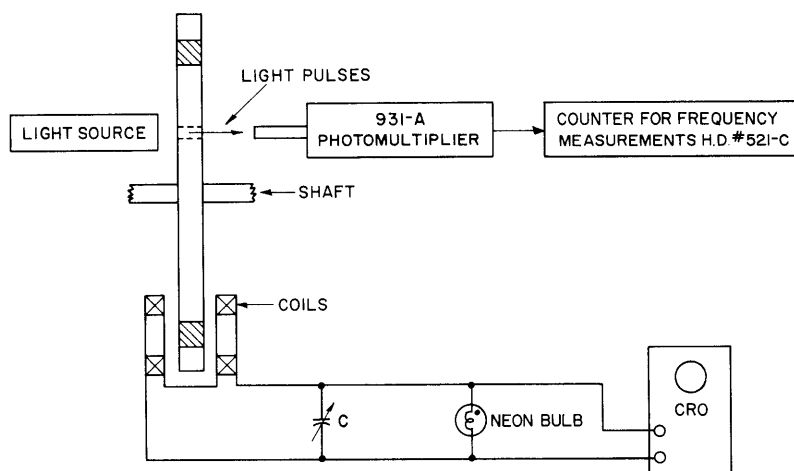


Fig. XVI-6. Experimental circuit for self-excitation measurements.

The expression for G_e that is given above is one-half that given in our earlier report. This expression gives better agreement between the model and parametric experiments and is qualitatively justifiable on the grounds that G_{max} is measured

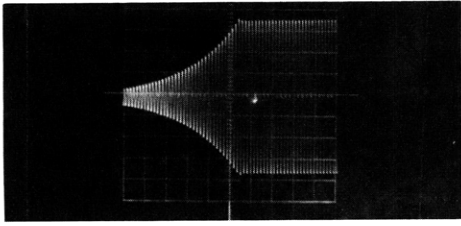


Fig. XVI-7. Oscilloscope trace showing voltage build-up for the self-excited system.

with the slug most tightly coupled with the coils, whereas in parametric operation the slugs spend as much time out of the coils as they do in the coils.

It is evident from the results of Table XVI-1 that exact prediction of self-excitation is not obtained according to Eq. 2; however, the relative prediction is shown to be good by experimental data.

The build-up of voltage for the self-excited system is shown in the oscilloscope trace of Fig. XVI-7. This experiment was performed with the circuit of Fig. XVI-6. The capacitance was shorted to make the output voltage zero. The oscilloscope trace was started by removing the short from the capacitor. The initial voltage amplitude is due to residual flux in the iron core. The voltage amplitude builds up approximately exponentially until the neon bulb ignites and thus limits the voltage.

In order to check the model further, additional measurements were made by connecting an external conductance (G_{ext}) in shunt with capacitor C, shown in Fig. XVI-6, and determining the external conductance that is necessary to stop self-excitation. This measurement was made with the 1-3 and 1-4 coil combinations (see Fig. XVI-4 and Table XVI-1) at various frequencies. The results are shown plotted in Fig. XVI-8.

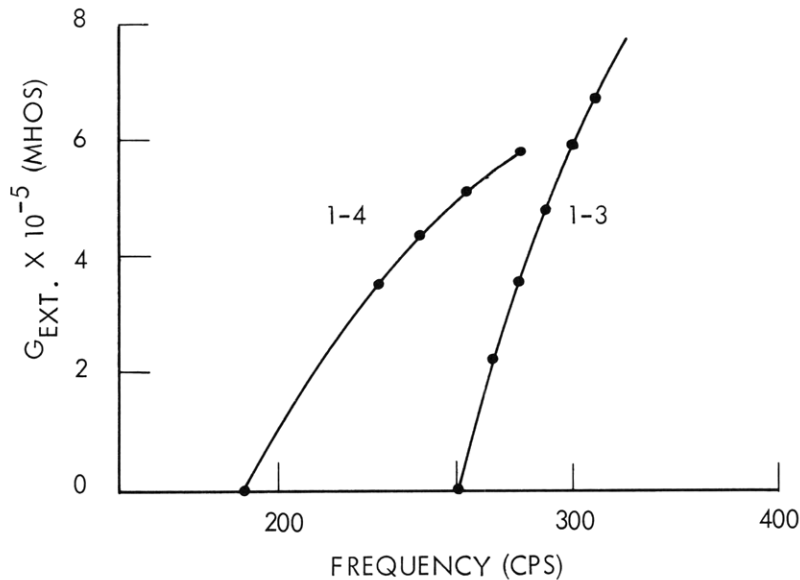


Fig. XVI-8. External conductance for threshold of self-excitation

(XVI. PLASMA MAGNETOHYDRODYNAMICS)

Table XVI-2. Data from Measurements Made to Check the Model

Frequency (cps)	Coil Combination	G_{ext} (10^{-5} mhos)	H
258	1-3	0	.67
270	1-3	2.2	.70
280	1-3	3.6	.69
290	1-3	4.8	.69
300	1-3	5.9	.71
188	1-4	0	.67
229	1-4	3.5	.70
262	1-4	5.3	.72

For each of the data points of Fig. XVI-8 for the 1-3 combination, steady-state ac measurements were made with the wheel at rest to determine the parameters and calculate a value of H (Eq. 2). The results are shown, together with some calculations for the 1-4 coil, in Table XVI-2. The results show that $H \geq 0.7$ is a good criterion for self-excitation for this geometry over the frequency range covered.

G. L. Wilson, A. T. Lewis, H. H. Woodson

C. FURTHER RESULTS OF VELOCITY-PROFILE MEASUREMENTS

This report is a summary of work done on velocity-profile measurements of mercury flowing in closed channels during the last quarter and reported in detail in the author's thesis.^{1, 2} During previous operation a large accumulation of oxides that appeared to be oxides of mercury collected in the system. Before work on velocity profiles was started again, considerable time was devoted to cleaning the system and washing the mercury. We also spent time on constructing an improved and sturdier circular test section (a similar square cross-section channel had been built previously) and in refurbishing the flow circuit. Then a detailed examination of the natural-rubber vacuum tubing, which is used to interconnect the various sections, was made. No deterioration of the inner walls which could be due to contact with flowing mercury was detected.

Once the system was again in operation, attention was given to better methods of stabilizing the probe against buoyant forces. Various mechanical systems were tried with little success, largely because of "stick-slip" problems during traverses and difficulties in accurately centering the probe. On the advice of D. A. East, the length of the probe mount was eventually reduced from 6 inches to 2 inches. The shorter length alone gave enough stability and no additional stiffening was required. It did not appear

to cause any problems resulting from disturbed flow near the traversing box. In current practice in fluid mechanics very short probes have been used, apparently, with good results.

During the period when the system was being cleaned, two improved traversing boxes were built. These allowed better sealing and closer control of the probe position.

While various probe configurations were being tested, the phenomenon of voltage reversal, which had been reported previously, again appeared. The difficulty, this time, was definitely traced to intermittent short circuits between the lead wires and the hollow steel mounting tube through which the probes ran. In probes that were constructed subsequently, greater care was taken to avoid damaging the enamel insulated wires as they were being inserted into the mounting tube.

The method of attaching the sensing head to the probe was changed to include an offset of approximately $3/32$ inch in the direction of traverse. This was done in order to bring the sensing head up against the wall on one side. This modification also gave an increased hydrodynamic efficiency that resulted in somewhat higher fluid velocities in the probe and therefore in higher voltages.

In most of the tests that were made, it became evident that the fluid velocity in the probe was now very nearly the same as that in the channel. This means that there was no significant resistance offered to the flow by the probe, and therefore there was little local distortion of the flow pattern. The existence of an average velocity inside the probe which was very nearly that of the local free stream also implies little boundary-layer formation inside.

Shielded probes were made with either insulators or conductors used for the shield.

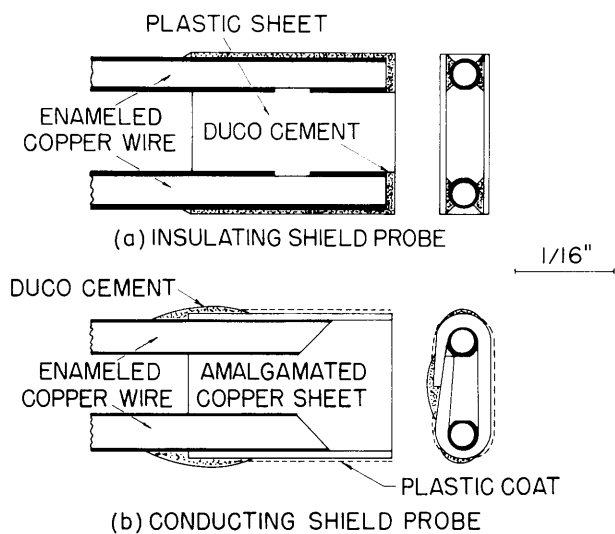


Fig. XVI-9. Typical velocity probes.

Probes with conducting shields were made which were very similar to those used previously. That is, a sheet of copper, 0.002 inch thick, was amalgamated with mercury on one side, coated with plastic on the other, cut into thin strips, rolled into a cylinder, and slipped over the pickup wires. (Fig. XVI-9b.) Probes with insulating shields were constructed by gluing thin sheets of plastic to the pickup wires to form a rectangular box. Each probe was checked out with an ohmmeter before it was used to ensure continuity and freedom from short circuits or electrical leaks.

(XVI. PLASMA MAGNETOHYDRODYNAMICS)

The probes were calibrated by setting them in the center of the channel, varying the average velocity, as indicated by the venturi meter, and reading the probe voltage. Velocities up to 160 cm/sec were used, which resulted in voltages as high as 400 μ v. The maximum velocity was limited by the finite length of the venturi manometer. All of the data were taken with turbulent flow in the channel.

A number of measurements of this kind were made; the results indicated some previously unobserved behavior. The first phenomenon is illustrated in Fig. XVI-10b. This represents a calibration of a Kolin type of probe with a conducting shield. There is a sudden and repeatable jump in the calibration curves. This jump takes place at the appropriate Reynolds number which is based on the probe hydraulic radius even though the flow in the main channel is turbulent. We may then conclude that the flow inside the probe is completely laminar below the jump, and turbulent after the jump. The two parts of the calibration curves have nearly the same slope, but the nonzero intercept is not explained.

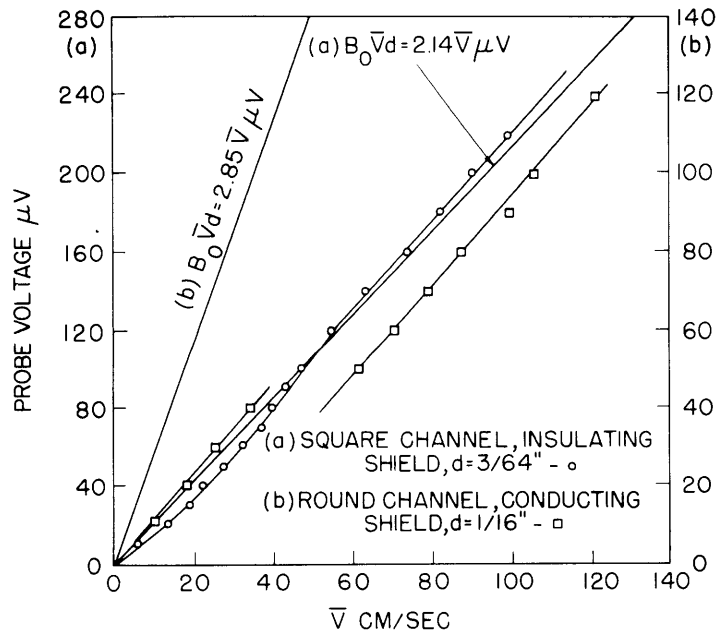


Fig. XVI-10. Probe calibrations ($B_0 = 1850$ gauss).

A second phenomenon is illustrated by Fig. XVI-10a. Here the flow seems to have remained laminar, but a decided curvature, which is not due to velocity-profile effects, has appeared. This curvature is repeatable at low velocities and showed up in several of the probes that were constructed.

It should be noticed that in the calibration runs shown here, the sensitivity of the

probes that were constructed with insulating shields is higher than that of those with conducting shields. In fact, probes made with insulating shields have a sensitivity that is very close to that predicted from the electrode spacing, magnetic field, and free-stream velocity. This is the basis of our contention that the average velocity of fluid in the probe is the same as that in the stream at the point where the probe is located. The smaller sensitivity of probes made with conducting shields may be explained by the shunting effect of the shield, which is also seen in electromagnetic flowmeters.

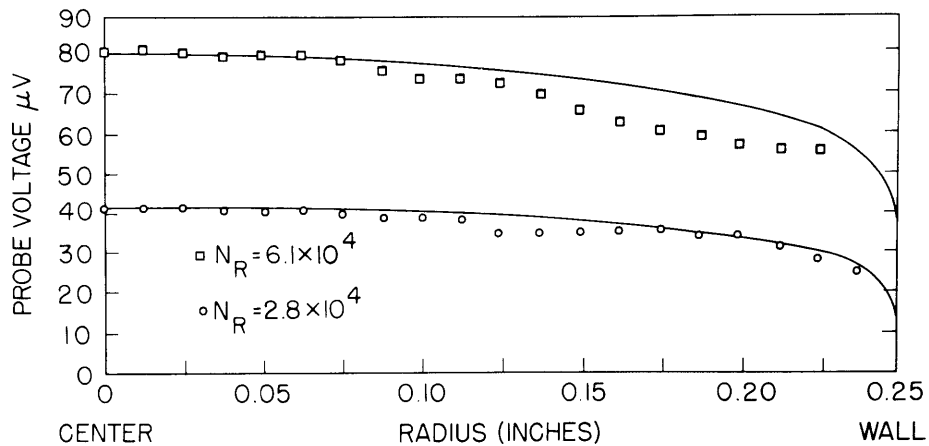


Fig. XVI-11. Velocity profiles (round channel, insulating shield).

Figure XVI-11 illustrates the result of probe traverses in turbulent flow, and conventional logarithmic profiles are presented for comparison. Several things may be noticed. (a) There is general agreement over much of the channel width with the long profile. (b) Serious deviations occur when the probe approaches the wall. The point at which this happens is approximately one probe thickness from the wall. (c) There is considerable variation in the flow rate during the traverse. (d) The profile flattens markedly before the probe nears the wall. This could conceivably be due to an actual deviation from the logarithmic profile, which is caused by a nonzero velocity at the wall as a consequence of its not being wet by mercury.

The following conclusions can be drawn from these data:

- a. The electromagnetic-probe method can be made to work.
- b. For maximum sensitivity, the probe should be made with insulating shields.
- c. The probe thickness must be made much smaller, in order to see the significant details of the velocity profile in the present flow circuit.
- d. It is imperative to have a better regulated flow system.

(XVI. PLASMA MAGNETOHYDRODYNAMICS)

e. There are some previously unrecognized aspects of probe behavior and channel flow which are worthy of further investigation.

G. B. Kliman

References

1. G. B. Kliman, Velocity Profiles in Hydromagnetic Channel Flow, S.M. Thesis, Department of Electrical Engineering, M.I.T., 1959.
2. G. B. Kliman, Velocity Profile Measurements, WADD Technical Report 60-148, edited by H. H. Woodson and W. D. Jackson, February 1960, pp. 35-52.

D. MAGNETOHYDRODYNAMIC AND ELECTROHYDRODYNAMIC SURFACE SHOCKS AND ANTISHOCKS

Many of the most interesting phenomena observed on fluid surfaces are essentially nonlinear in character. Breakers at the beach or hydraulic jumps at the foot of a dam are waves that are strongly influenced by a velocity of propagation that depends on the fluid depth. The breaker is a form of surface shock.

Magnetohydrodynamic and electrohydrodynamic surface waves have phase velocities that are directly dependent on the electric and magnetic field intensities, just as long gravity waves depend directly for their velocity on the square root of the depth. It would be expected that nonlinear stages of the surface interactions that have been described by the author elsewhere¹ could be discussed in a way that is similar to that commonly used in the literature concerned with gravity waves.² It is the purpose of this report to outline the reduction of two simple surface-wave problems to a tractable but nonlinear form. The dynamics described by the resulting equations are illustrated by means of several transient examples and the corresponding shock relations are derived.

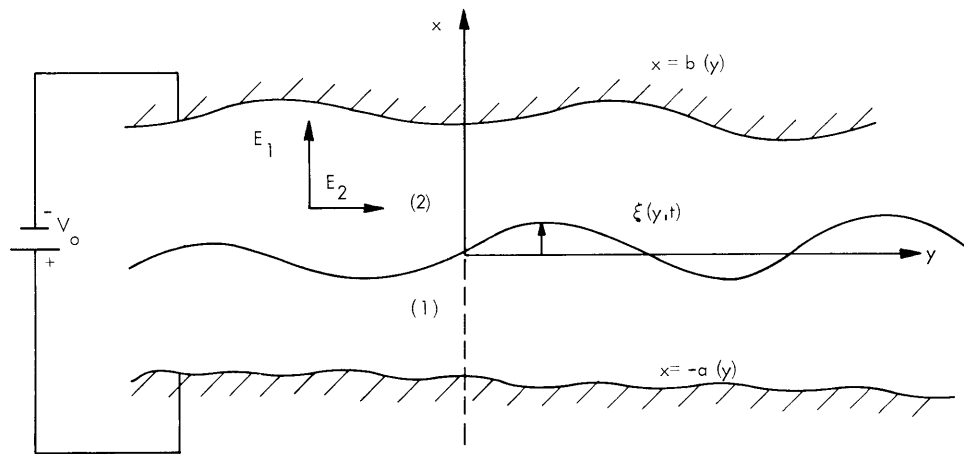


Fig. XVI-12. Electrohydrodynamic configuration.

1. Electrohydrodynamic Wave

The problem to be considered here is illustrated by Fig. XVI-12. A shallow conducting fluid is stressed by a perpendicular field and bounded above by a fluid of small density (water and air, for example). The fluid is confined from below by a surface at $x = -a(y)$, and the potential at $x = b(y)$ is constrained to $-V_0$ with respect to the conducting fluid. A gravitational field acts in the negative x direction. The pertinent bulk equations are:

$$\rho \left[\frac{\partial \bar{V}}{\partial t} + (\bar{V} \cdot \nabla) \bar{V} \right] + \nabla p' = 0 \quad (1)$$

where $p' = (p + \rho gx)$,

$$\nabla \cdot \bar{V} = 0 \quad \nabla \times \bar{V} = 0 \quad (2)$$

$$\nabla \cdot \bar{E} = 0 \quad \nabla \times \bar{E} = 0 \quad (3)$$

where ρ is fluid density, \bar{V} is fluid velocity (components, V_1, V_2, V_3), p is fluid pressure, g is the gravitational constant, and \bar{E} is the electric field intensity. Boundary conditions consistent with these equations are:

$$[n_\alpha p - T_{\alpha\beta} n_\beta]_{x=\xi(y,t)} = 0 \quad (4)$$

where ξ represents the fluid interface position, and $T_{\alpha\beta} = \epsilon E_\alpha E_\beta - \delta_{\alpha\beta} \frac{\epsilon}{2} E_\gamma E_\gamma$, with ϵ representing the permittivity of free space.

$$[\bar{n} \cdot \bar{V}]_{x=-a(y)} = 0 \quad (5)$$

$$\int_{\xi}^b E_1 dx = V_0 \quad (6)$$

$$[\bar{n} \times \bar{E}]_{x=\xi} = 0 \quad (7)$$

Also, the interface is defined dynamically and geometrically by

$$\frac{DF}{Dt} = \left[-\frac{\partial \xi}{\partial t} + V_1 - V_2 \frac{\partial \xi}{\partial y} \right]_{x=\xi(y,t)} = 0 \quad (8)$$

$$\bar{n} = \frac{\nabla F}{(\nabla F \cdot \nabla F)^{1/2}} = \left[\bar{a}_1 - \bar{a}_2 \frac{\partial \xi}{\partial y} \right] \left[1 + \frac{\partial \xi}{\partial y} \right]^{-1/2} \quad (9)$$

where $F = x - \xi(y, t)$.

Equations 8 and 9 may be used to restate the boundary conditions of Eqs. 5 and 7.

(XVI. PLASMA MAGNETOHYDRODYNAMICS)

$$\left[V_1 + V_2 \frac{\partial a}{\partial y} \right]_{x=-a(y)} = 0 \quad (10)$$

$$\left[E_2 + \frac{\partial \xi}{\partial y} E_1 \right]_{x=\xi(y,t)} = 0 \quad (11)$$

Differentiate Eq. 6 with respect to y , and use Eq. 11 to write

$$\left[E_2 + \frac{\partial b}{\partial y} E_1 \right]_{x=b(y)} = 0 \quad (12)$$

Equation 11 and the two nontrivial equations of Eq. 4 can be combined:

$$\left[p + \frac{\epsilon E_1^2}{2} \left(1 + \left(\frac{\partial \xi}{\partial y} \right)^2 \right) \right]_{x=\xi(y,t)} = 0 \quad (13)$$

The pertinent equations are now Eqs. 1, 2, 3, 8, 10, 11, 12, and 13.

An approximation to these equations is now to be formulated, based upon an expansion in a "space rate" parameter. This parameter, which has the effect of scaling the width-to-depth ratio, will be taken as $\lambda = \left(\frac{w}{s} \right)^2$, with w and s representing the characteristic vertical and horizontal dimensions, respectively. The dimensionless variables are:

$$\begin{aligned} y &= \bar{y}s & V_1 &= \bar{V}_1 \sqrt{gw} \left(\frac{s}{w} \right) & \bar{b} &= bw \\ x &= \bar{x}w & V_2 &= \bar{V}_2 \sqrt{gw} & a &= \bar{a}w \\ t &= \frac{\bar{t}s}{\sqrt{gw}} & p &= \bar{p}\rho gw & E_1 &= E_o \bar{E}_1 \\ & & \xi &= \bar{\xi}w & E_2 &= E_o \left(\frac{s}{w} \right) \bar{E}_2 \\ & & & & wE_o \bar{V}_o &= V_o \end{aligned}$$

The time has been purposely scaled to horizontal distances, while the velocity is scaled to the velocity of gravity waves. The vertical velocity and y -directed electric field have been intentionally suppressed by the ratio (s/w) . This normalization has the effect of making the first terms in the λ expansion physically meaningful when a and b are small compared with the curvature of the surface.

A series solution for each of the dependent variables is now assumed to be of the form

$$\bar{V}_1 = \frac{0}{\bar{V}_1} + \lambda \frac{1}{\bar{V}_1} + \lambda^2 \frac{2}{\bar{V}_1} + \dots \quad (14)$$

The normalized equations of motion are required to be satisfied to all orders of λ . The zero-order equations may be integrated to define first-order equations that, in turn, are taken as the equations of motion. These are written:

$$\frac{\partial \bar{V}_2}{\partial \bar{t}} + \bar{V}_2 \frac{\partial \bar{V}_2}{\partial \bar{y}} + \frac{\partial \bar{\xi}}{\partial \bar{y}} + \frac{U_b^2 V_o^2}{(\bar{b} - \bar{\xi})^3} \frac{\partial (\bar{b} - \bar{\xi})}{\partial y} = 0 \quad (15)$$

$$\frac{\partial \bar{\xi}}{\partial \bar{t}} + \frac{\partial (\bar{V}_2 (\bar{\xi} + \bar{a}))}{\partial \bar{y}} = 0 \quad (16)$$

$$\bar{E}_1 = \bar{V}_o(t) / (\bar{b} - \bar{\xi}) \quad (17)$$

$$U_b^2 = \epsilon E_o^2 / \rho g w .$$

2. Magnetohydrodynamic Antidual

The magnetohydrodynamic problem of a flux of magnetic field trapped between a rigid perfectly conducting wall at $x = b(y)$ and a perfectly conducting fluid interface at $x = \xi(y, t)$ can be shown to be very similar to the problem outlined in the previous section. This problem is summarized in Fig. XVI-13.

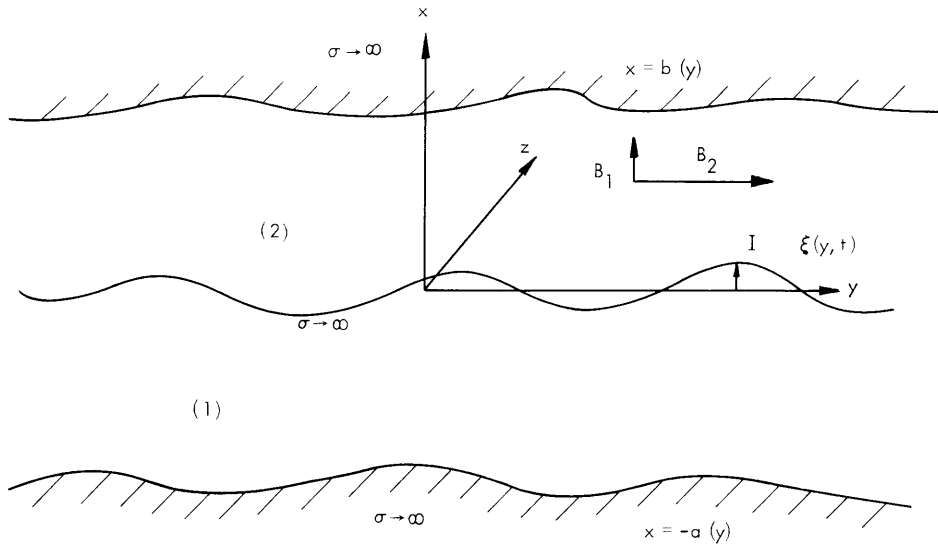


Fig. XVI-13. Magnetohydrodynamic configuration.

(XVI. PLASMA MAGNETOHYDRODYNAMICS)

Since the magnetic field is presumed to be confined to region (2), the fluid bulk equations are given by Eqs. 1 and 2. However, induction is essential, so that

$$\nabla \times \mathbf{E} = -\frac{\partial \mathbf{B}}{\partial t} \quad (18)$$

$$\nabla \cdot \mathbf{B} = 0 \quad (19)$$

$$\nabla \times \mathbf{B} = 0 \quad (20)$$

where \mathbf{B} is the magnetic field intensity. These equations apply in region (2).

The boundary conditions of Eqs. 10 and 11 are applicable, while the conditions that replace Eqs. 6 and 7 are:

$$\int_{\xi(y,t)}^{b(y)} B_2 dx = \Lambda_0 \quad (21)$$

$$[\bar{\mathbf{n}} \cdot \bar{\mathbf{B}}]_{x=\xi(y,t)} = 0 \quad (22)$$

Also, Eq. 18 requires that

$$\bar{\mathbf{n}} \times [\mathbf{E}^{(2)} - \mathbf{E}^{(1)}]_{x=\xi(y,t)} = \bar{\mathbf{n}} \cdot \bar{\nabla} [\mathbf{B}^{(2)} - \mathbf{B}^{(1)}]_{x=\xi(y,t)} \quad (23)$$

If the induced electric field \mathbf{E}_3 exists, the surface charge must vanish. Hence, the surface traction is accounted for by the magnetic counterpart of the stress tensor in Eq. 4.

Equation 20 shows that B_3 may be taken as zero. Therefore, Eq. 4 gives

$$\left[p - \frac{B_2^2}{2\mu} \left[1 + \left(\frac{\partial \xi}{\partial y} \right)^2 \right] \right]_{x=\xi(y,t)} = 0 \quad (24)$$

where μ is the permeability of free space.

The problem is now defined by the volume equations (1), (2), (19), and (20), together with the surface conditions of (8), (10), (21), (22), and (24).

In the same way as in section 1, a solution in the form of a power series in λ is assumed, and equations are found to first order in λ . However, here the magnetic field is scaled so that $B_1 = B_0 \bar{B}_1 (s/w)$, $B_2 = B_0 \bar{B}_2$. Following the line of rationalization used previously, we find that the equations of motion are given by Eqs. 15, 16, and 17 after the substitution

$$\bar{\mathbf{V}}_0 \rightarrow \bar{\Lambda}_0$$

$$U_b^2 V_0^2 \rightarrow -\bar{U}_a^2 \Lambda_0^2$$

$$\mathbf{E}_1 \rightarrow \mathbf{B}_2$$

where $U_a^2 = \frac{B_o^2}{\mu\rho g w}$.

The change of sign in going from U_a^2 to U_b^2 is the basis for calling the problems of sections 1 and 3 antiduals. The effect of this sign change on physical problems will be apparent in the rest of this report.

3. Characteristic Equations

The characteristic equations that are equivalent to Eqs. 15 and 16 are found by using standard techniques.³ (It is assumed, now, that $a(y) = a, b(y) = b$, or that the boundaries are parallel.) Designating the families of characteristics in the y - t plane as C^+ and C^- , we have:

$$\left. \begin{array}{l} C^+ \quad V' + R(\phi, K) = c_1 \\ C^- \quad V' - R(\phi, K) = c_2 \end{array} \right\} \quad (25)$$

where c_1 and c_2 are constants,

$$\left. \begin{array}{l} C^+ \quad \frac{dy'}{dt} = V' + \sqrt{(1-\phi)(1-K/\phi^3)} \\ C^- \quad \frac{dy'}{dt} = V' - \sqrt{(1-\phi)(1-K/\phi^3)} \end{array} \right\} \quad (26)$$

In Eqs. 25 and 26,

$$R(\phi, K) = - \int_{\text{constant}}^{\phi} \left[\frac{\phi^3 - K}{\phi^3(1-\phi)} \right]^{1/2} d\phi \quad (27)$$

$$V' = \bar{V}_2 / \sqrt{\bar{a} + \bar{b}}$$

$$y' = \bar{y} / \sqrt{\bar{a} + \bar{b}}$$

$$\phi = \left| \frac{\bar{b} - \bar{\xi}}{\bar{b} + \bar{a}} \right|$$

$$K = U_b^2 V_o^2 / (b+a)^3 \quad \text{or} \quad -U_a^2 \Lambda_o^2 / (b+a)^3$$

Since Eq. 26 is complex if $k/\phi^3 > 1$ ($\phi > 1$ is not physically meaningful), this is the condition that real characteristics exist, and hence that the equations be hyperbolic. In the linear theory, this is also the condition that the interface be stable.¹ The two

(XVI. PLASMA MAGNETOHYDRODYNAMICS)

theories agree with respect to the definition of stability if, as we shall do here, the nonlinear unstable interface is taken to be one that is no longer defined by hyperbolic differential equations.

Solutions starting from $\phi^3 > K$ will be shown to tend to remain in this condition. Hence this is a plausible and consistent definition if used in connection with this first-order theory.

4. The Growth of Shocks and Antishocks

a. Simple Waves

The problem of a wave propagating into a region of constant state ($v' = 0, \phi = \phi_0$), defined by its height for time $t > 0$ at a fixed position, is easily investigated, since all of the characteristics of one family (say, the C^+) intersect at some point characteristics that originate in a region of constant state. Equations 25 and 26 imply that ϕ and v' are constant along C^+ characteristics and that these are straight lines. Only $\phi|_y = 0$ as a function of time need be given because, from Eq. 25,

$$V|_{y=0} = R(\phi, K)|_{y=0} - R(\phi_0, K).$$

Hence the characteristics are easily drawn by using Eq. 26 to determine the slopes. That is, the C^+ characteristics intersect the time axis with a slope given by

$$M = \frac{dy'}{dt} = \left[R(\phi, K) - R(\phi_0, K) + \sqrt{(1-\phi)(1-K/\phi^3)} \right]_{y=0} \quad (28)$$

Clearly, if this slope increases with increasing time, the C^+ characteristics must cross and the wave must steepen into a shock. Hence, the condition

$$\left[\frac{dM}{d\phi} \frac{d\phi}{dt} \right]_{y=0} > 0 \quad (29)$$

implies that a shock will form. Equations 27 and 28 show that

$$K \gtrsim \phi^4 \quad \text{implies} \quad \frac{dM}{d\phi} \gtrsim 0.$$

Four possible dynamical situations are of interest.

1. Magnetohydrodynamic compression waves: $\frac{d\phi}{dt} < 0, K < 0, \frac{dM}{d\phi} < 0$; in this case a shock will always form.
2. Magnetohydrodynamic depression wave: $\frac{d\phi}{dt} > 0, K < 0, \frac{dM}{d\phi} < 0$; in this case a shock will never form.
3. Electrohydrodynamic compression wave: $\frac{d\phi}{dt} < 0, K > 0, \phi^3 > K$ for stability.

A shock may or may not form: (a) $\phi^4 < K < \phi^3$, in which case $\frac{dM}{d\phi} > 0$, or a shock does not form; (b) $\phi^4 > K$ or $\frac{dM}{d\phi} < 0$, in which case a shock forms.

4. Electrohydrodynamic depression wave: $\frac{d\phi}{dt} > 0$, $K > 0$. A shock may or may not form: (a) $\phi^4 < K < \phi^3$ or $\frac{dM}{d\phi} > 0$, in which case a shock forms; (b) $\phi^4 > K$ or $\frac{dM}{d\phi} < 0$, in which case a shock does not form.

These statements apply strictly only to waves with corresponding values of ϕ confined to a single regime. For waves that make a transition from one regime to another, the negative statements would be that a shock does not tend to form, the reason being that, while the C^+ characteristics may be spreading with increasing time, they may still cross characteristics in another regime, although at a later time, than they would if the spreading had not occurred.

A transition compression wave would tend to form into a shock at its base while smoothing out at its top. Similarly, a transition depression wave would form a discontinuity near the initial wave front and smooth out at the back of the wave. These are reasonable consequences of the tendency of the wave velocity to increase with increasing depth because of the gravitational field, and to decrease with increasing depth because of the electric field. The dynamics are roughly the same as for ordinary gravity waves, as long as $\phi^4 > K$. Hence this regime will be called "gravity-controlled," and $\phi^4 < K < \phi^3$ will be called "E-H-D controlled."

As examples of E-H-D transition waves, Figs. XVI-17 and XVI-18 show the compression and depression waves of Fig. XVI-14 propagating into regions of constant state. The associated characteristics are given in Figs. XVI-15 and XVI-16.

Since the dynamics of the magnetohydrodynamic simple waves is not grossly different from that of ordinary gravity waves, we shall simply point out that the effect of a magnetic field is always to make a compression wave shock occur earlier in time, since increasing the magnetic field has the effect of making $dM/d\phi$ more negative.

Although the discontinuities formed by E-H-D controlled waves may be called shocks, it would seem to be worth while to draw attention to the fact that their behavior is just the opposite of shocks normally formed in nature by referring to them as "antishocks." Here the shock is associated with the wavelike property of a system, while the antishock is a consequence of a tendency toward instability. The antishock should not, however, be confused with the manifestation of an instability.

b. Waves from Spacelike Data

It is interesting to briefly consider certain disturbances that originate on initial static displacements of the interface. That is, given that $V = 0$ and $\xi = \xi_1(y)$ at $t = 0$, what is the ensuing dynamical motion?

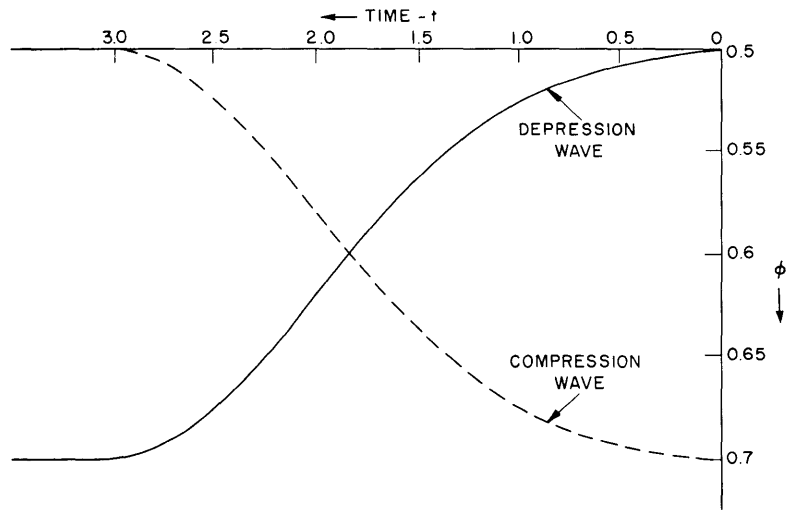


Fig. XVI-14. Timelike wave.

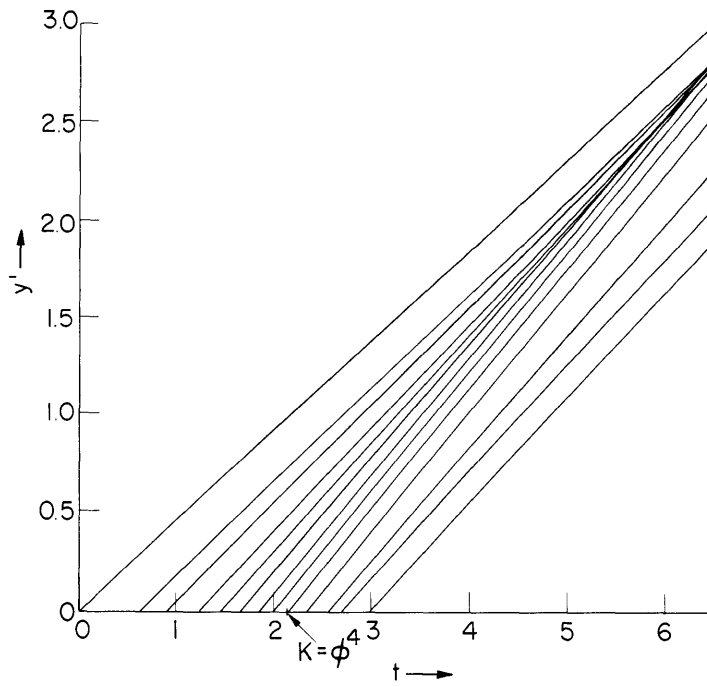


Fig. XVI-15. Characteristics for compression E-H wave.

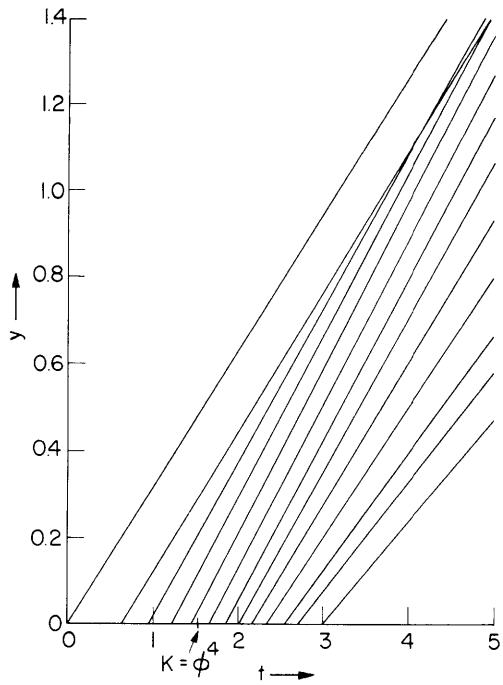


Fig. XVI-16. Characteristics for depression E-H wave.

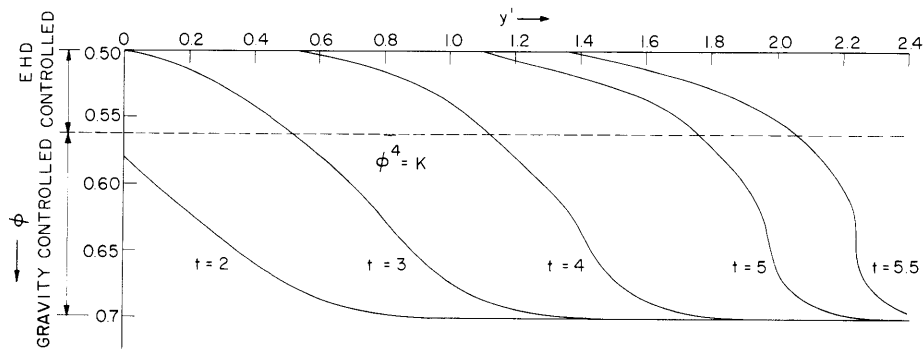


Fig. XVI-17. E-H transition compression wave.

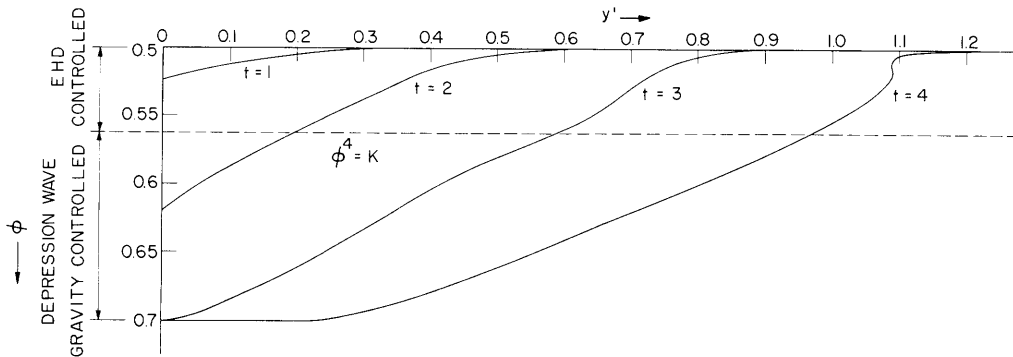


Fig. XVI-18. E-H transition depression wave.

(XVI. PLASMA MAGNETOHYDRODYNAMICS)

Equations 25, 26 and 27 make possible, in the usual way, a stepwise construction of the characteristics and hence of the solution. Interest is confined here to pulses that are symmetrical about the origin and bounded by regions of constant state. Hence, the problem is completely solved for $t \geq 0$ by

(a) Performing the integral of Eq. 27 to determine the values of c_1 and c_2 from the initial data for characteristics originating at intervals along the y axis in the region of the pulse;

(b) Simultaneously solving Eqs. 25 and inverting $R(\phi, K)$ to determine ϕ and V at all characteristic intersections in a region bounded by the y axis and the C^+ and C^- characteristics originating from the negative and positive y extremities of the initial pulse;

(c) Iteratively using the characteristic directions defined by Eq. 26 to determine the (y, t) position corresponding to each of the characteristic intersections of 2.

The problem is solved for all y and t once the characteristics have been determined in the "cone" of part 2, since all characteristics leaving the region are straight lines. (They intersect characteristics the originate in a region of constant state.)

A problem, pertinent to the effect of finite surface displacements on impending instability, can be resolved from the simple fact that $R(\phi, K)$ is a negative monotonically decreasing function of ϕ . The fact that any initial static displacement of the interface that is stable will remain stable follows from Eq. 25. Let ϕ_0 be the minimum value of ϕ at $t = 0$ and for $y = y_0$. Then originating at ϕ there are C^+ and C^- characteristics along which

$$V' \pm R(\phi, K) = \pm R(\phi_0, K). \quad (30)$$

Similarly, along characteristics originating at another arbitrary point y_1 , we have

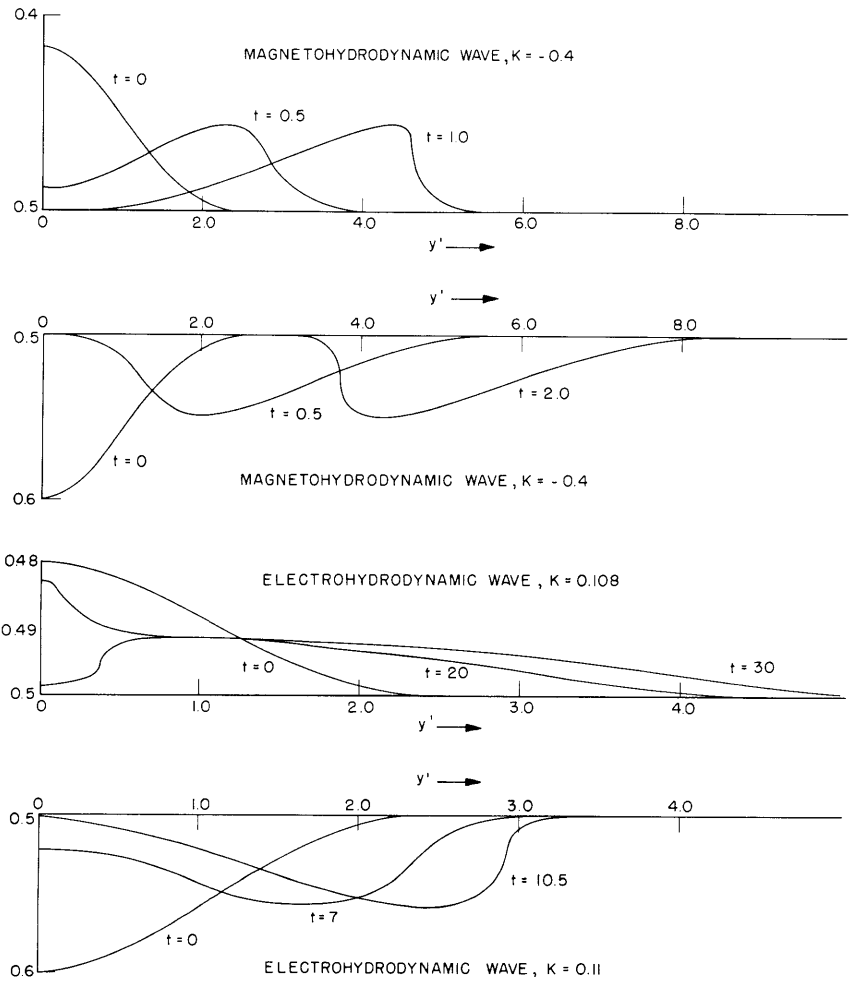
$$V' \pm R(\phi, K) = \pm R(\phi_1, K), \quad (31)$$

where $\phi_1 > \phi_0$. Therefore at any given point on the characteristics coming from y_0 there is a ϕ_1 that is such that

$$R(\phi, K) = [R(\phi_0, K) + R(\phi_1, K)] / 2, \quad (32)$$

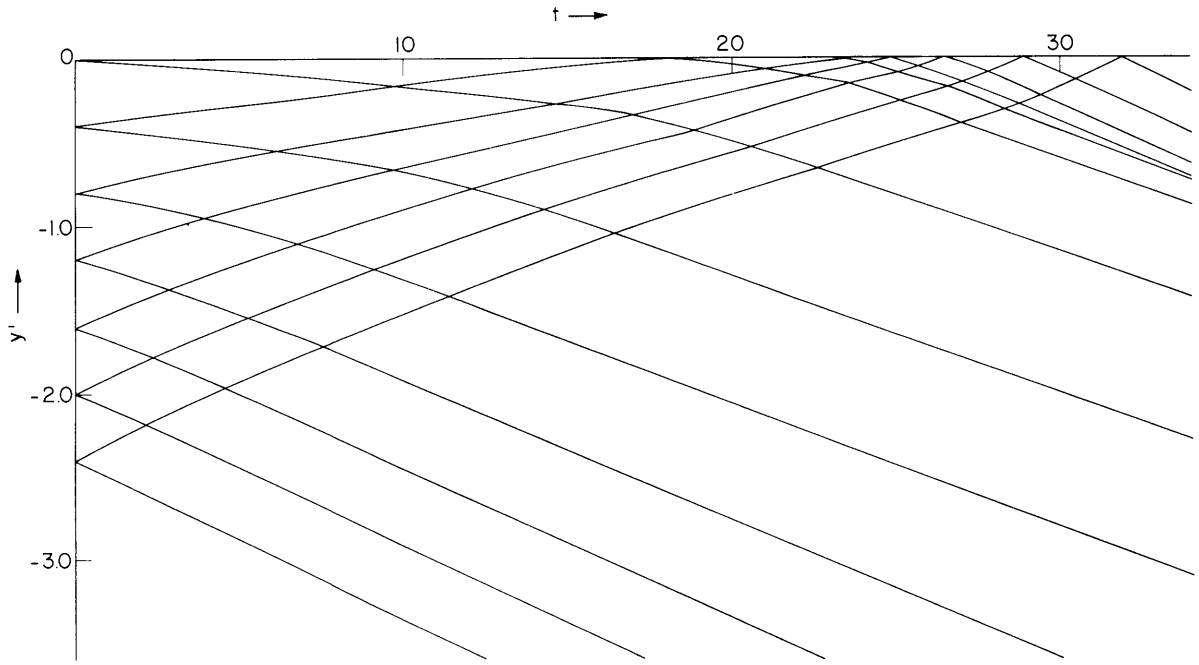
or since $R(\phi_0, K) > R(\phi_1, K)$, $R(\phi, K) < R(\phi_0, K)$, and $\phi > \phi_0$ along the y_0 characteristics originating in y_0 . The argument is complete if it is observed from Eq. 32 that ϕ takes on the smallest possible values on the characteristics that cross at y_0 . Hence, ϕ is greater than ϕ_0 everywhere in the $(y, t > 0)$ plane and the interface remains stable.

As examples of symmetric waves originating on initially static pulses, Fig. XVI-19 shows magnetohydrodynamic and electrohydrodynamic hump and depression pulses propagating into regions of constant state. Since the resulting waves are symmetric about the origin, only the positive y axis is shown. In these examples the electrohydrodynamic



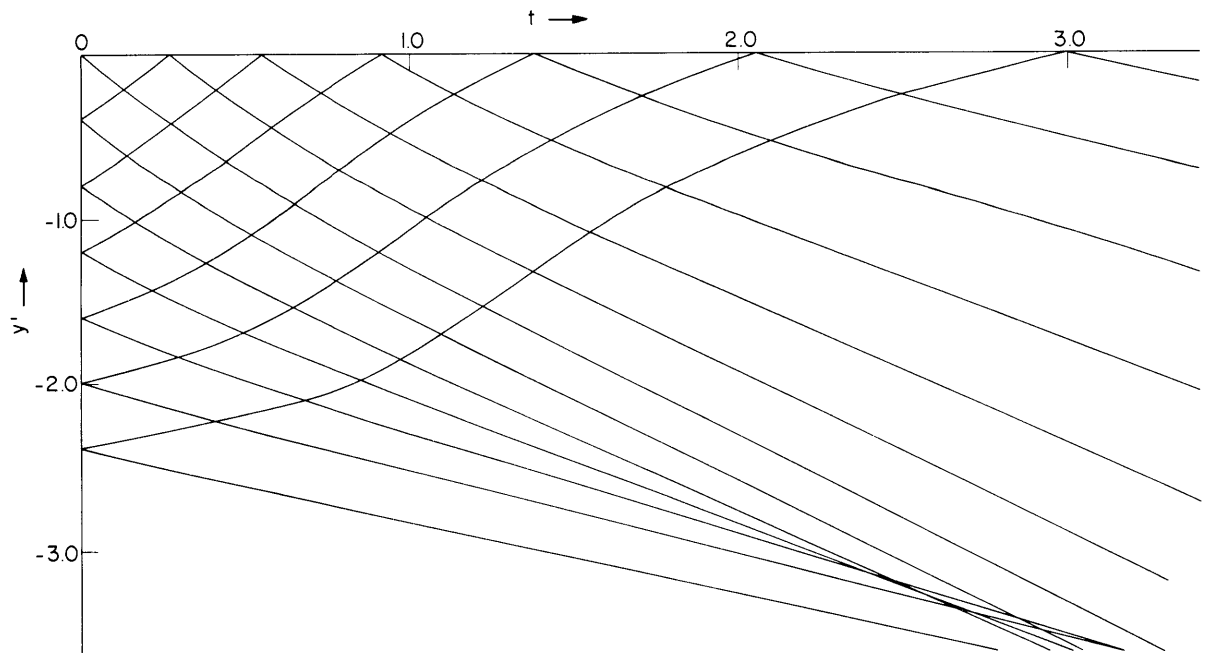
(a)

Fig. XVI-19(a). Waves from spacelike data.



(b)

Fig. XVI-19(b). E-H characteristics of the compression wave.



(c)

Fig. XVI-19(c). E-H characteristics of the depression wave.

cases do not make a transition to the gravity-controlled regime.

The waves behave as would be expected. The velocity of small disturbances increases with the depth of the fluid in the magnetohydrodynamic problem. The particles at the top of the hump catch up with those at the front, while the particles at the back of a depression catch up with those at the bottom. Hence in a way similar to the ordinary gravity wave, a hump steepens into a shock at the front and a depression forms a shock at its back edge.

Conversely, the velocity of small disturbances can decrease with the fluid depth for an electrohydrodynamic problem. Hence, in the examples shown, antishocks form at the back and front edges of the hump and depression waves, respectively.

5. Integral Conditions

The conditions for fully developed shocks may be written by integrating the first-order equations over a volume that encloses the shock. The appropriate volume element is shown in Fig. XVI-20 for the electrohydrodynamic and magnetohydrodynamic cases.

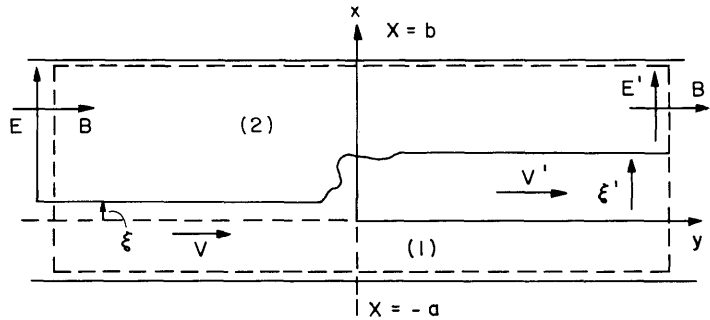


Fig. XVI-20. Shock configuration.

Note that the upper and lower boundaries of the volume are just inside the rigid parallel plates. The fluid is assumed to enter and leave the volume with velocities v and v' as shown. The problem is assumed to be steady-state, that is, the discontinuity is fixed in position. The equations of motion are invariant to a constant translation. Hence the problem is easily generalized to give a moving discontinuity. Since $\frac{\rho}{V_2} = \frac{\rho}{V_2}(y, t)$, the continuity condition requires that

$$V'(\xi'+a) = V(\xi+a) \quad (33)$$

From Eq. 17, the electric fields are related,

$$E(b-\xi) = E'(b-\xi') = V_0. \quad (34)$$

(XVI. PLASMA MAGNETOHYDRODYNAMICS)

The momentum equation (1) may be generalized to apply throughout the volume, as long as it is agreed that when it is taken in region (2), the density vanishes. That is,

$$\rho \left[\frac{\partial V_{\alpha}}{\partial t} + V_{\beta} \frac{\partial V_{\alpha}}{\partial x_{\beta}} \right] + \frac{\partial p}{\partial x_{\alpha}} = \frac{\partial(-\rho g x_1)}{\partial x_{\alpha}} + \frac{\partial T_{\alpha\beta}}{\partial x_{\beta}}. \quad (35)$$

A detailed knowledge of the field in the vicinity of the discontinuity is not known. However, far from the discontinuity it would be expected that the first-order field approximations would apply. Use may be made of these solutions to integrate Eq. 35 over the volume indicated in Fig. XVI-20. The volume integral of Eq. 35 is converted to a surface integral

$$\frac{\partial}{\partial t} \int_V \rho V_{\alpha} dv + \int_S \rho V_{\alpha} (V_{\beta} n_{\beta}) ds + \int_S p n_{\alpha} ds = \int_S T_{\alpha\beta} ds_{\beta}. \quad (36)$$

Since the volume was chosen so that there is no contribution to the integration of the y component of Eq. 36 on the upper and lower surfaces, the first-order fields serve to evaluate Eq. 36, and give

$$\rho [(\xi'+a)V'^2 - (\xi+a)V^2] + \frac{\rho g}{2} [(\xi'+a)^2 - (\xi+a)^2] - \frac{\epsilon}{2} [E'^2 [(\xi'+a) - (b-\xi')] - E^2 [(\xi+a) - (b-\xi)]] = 0 \quad (37)$$

Equations 33, 34, and 37 relate the velocity of the fluid into the volume to the discontinuity in the surface height.

$$V^2 = \frac{(\xi'+a)}{(\xi+a)} \left[\frac{g}{2} [(\xi'+a) + (\xi+a)] - \frac{\epsilon_0 V_0^2}{2\rho} \left(\frac{(\xi+a)(b-\xi') + (\xi'+a)(b-\xi)}{(b-\xi')^2 (b-\xi)^2} \right) \right] \quad (38)$$

The velocity of a wave front moving into a region of constant state is numerically equal to V. Hence, Eq. 38, for small ξ' and ξ , reduces to the phase velocity resulting from linear theory.¹

The shock conditions are fully formulated only after account is taken of the energy balance associated with a given discontinuity in the interface position. Since $\nabla \cdot V = 0$, the energy equation results from dotting V into Eq. 1 to obtain the condition

$$\frac{dw}{dt} = - \int_V \nabla \cdot (\bar{V}w) dv = - \int_S \bar{V}w \cdot ds, \quad (39)$$

where

$$w = \rho \left(\frac{V \cdot V}{2} \right) + p + \rho(x+a)$$

For a conservative system $dw/dt = 0$. At the shock front, kinetic energy may not be conserved. However, it is certainly true that in the physical system energy must

flow into the volume and not out of it. Hence the condition

$$\frac{dw}{dt} > 0$$

is required.

The integration of Eq. 39, carried out by using the value of V^2 given by Eq. 38, after some algebraic manipulations, yields

$$\frac{dw}{dt} = \frac{V(\xi' - \xi)^3}{4(\xi' + a)} \left\{ \rho g - \frac{(a+b)\epsilon_0 V_0^2}{[(b-a) - \xi]^2 [(b-a) - \xi']^2} \right\} \quad (40)$$

If $V_0 = 0$, this equation gives the well-known result that $V > 0$ implies that $\xi' > \xi$, or that the step in fluid height is as shown in Fig. XVI-20.

Equations 34, 38, and 40 hold for the magnetohydrodynamic problem of a trapped-magnetic field directed far from the discontinuity, along the y axis, if the substitution

$$E \rightarrow B$$

$$\epsilon_0 V_0^2 \rightarrow -\Lambda_0^2 / \mu$$

is made.

It is now clear that,

(a) A magnetohydrodynamic surface shock, like the gravitational shock, must propagate into a region of higher velocity and lower depth. That is, for $V > 0$ the energy balance requires $\xi' > \xi$.

(b) An electrohydrodynamic surface shock, unlike the gravitational shock, may propagate into a region of lower velocity and greater depth. That is, for $V > 0$ the energy balance does not require $\xi' > \xi$. In fact, it follows from Eq. 40 that the existence of a discontinuity does not necessarily imply that energy is dissipated at the interface.

These results are a consequence of the fact that the magnetic field always increases the equilibrium velocity of the discontinuity, while the electric field always decreases this velocity. It appears that the electric field may interact as an "electric weir," in that it may produce an abrupt decrease in the fluid depth in the stationary configuration of Fig. XVI-20.

The spacelike problems of section 5b were completed by use of the IBM 709 computer. This work was done at the Computation Center, Massachusetts Institute of Technology, Cambridge, Massachusetts.

J. R. Melcher

(XVI. PLASMA MAGNETOHYDRODYNAMICS)

References

1. J. R. Melcher, Electrohydrodynamic and magnetohydrodynamic surface waves and instabilities, *Phys. Fluids* 4, 11 (1961).
2. J. J. Stoker, The formation of breakers and bores, *Commun. Pure Appl. Math.* 1, 1 (1948).
3. R. Courant and K. O. Friedrichs, Supersonic Flow and Shock Waves (Interscience Publishers, Inc., New York, 1948), p. 40.